Modern Methods for Joint Analysis and Inversion of Geophysical Data

V.V. Spichak✉

Geoelectromagnetic Research Center of Schmidt Institute of Physics of the Earth, Russian Academy of Sciences,
Troitsk, Moscow, 108840, Russia

Abstract—This is an overview of existing methods for joint analysis and inversion of geophysical data, including conventional techniques and alternative options based on simultaneous and sequential inversion of different data sets and posterior analysis of separate inversion results. Advantages and disadvantages of different methods are compared using examples of typical cases, and the respective practical recommendations are provided for each method.

Keywords: Geophysical data, joint analysis, inversion, correlation, artificial neural network, cluster analysis

INTRODUCTION

Geophysical data have implications for lithology, petrology, or reservoir properties (saturation, porosity, permeability) of rocks, etc. These super-parameters are anyhow related with rock physical properties (conductivity, density, temperature, etc.) that can be determined explicitly or implicitly from measurable geophysical data. The interface between the model spaces of different levels is ensured with petrophysical and geostatistical data between the first-level model space and the data by forward modeling using the respective measured values (Fig. 1).

Independent models for specific data sets are obtained by different algorithms with reference to *a priori* geological and geophysical data. This kind of modeling often faces problems associated with

– low resolution of measured data with respect to target parameters;

– low accuracy and resolution of the models resulting from shortage and/or poor quality of measurements and priors;

– non-uniqueness and instability of inversion;

– poor efficiency of existing inversion algorithms (especially, in 3D/4D problems);

– lack of mechanisms for quantifying the prior and peer inspection results.

These problems are anyhow resolvable in inversion of some specific types of data. Yet, geologists or geophysicists often find the results unsatisfactory and try to reduce the uncertainty and thus improve the inversion quality by integrating data from different methods (Bedrosian, 2007; Spichak,

2009, 2010; Integrated…, 2016; Fullea, 2017). Researches try to obtain consistent and robust models of geological/geophysical systems by combining independent data sets, which often differ in physics, scale, resolution, quality, etc. This integration may be difficult as well, because the data sets

– may be measured in different areas and/or to different resolution;

– may differ in resolution with respect to the target parameters;

– may lead to rock properties/parameters that poorly correlate with one another, etc.

If these risks are neglected, joint inversion may deteriorate the results instead of improving them. However, researchers may even remain unaware of this loss in the real practice (rather than in a modeled situation), in the absence of objective criteria to judge whether the quality of joint inversion is better than inversion of independent data sets. Therefore, a critical review of approaches to data integration is of both academic and practical interest.

This overview offers a preliminary classification and comparative analysis of parallel and sequential inversion of geophysical data and posterior analysis of independent inversion results.

JOINT INVERSION

The idea of joint inversion consists in modeling the behavior of a parameter using all available data in order to reduce the ambiguity and improve the accuracy. Different models are built with the respective data set each and correlated with reference to *a priori* data (priors) introduced by the user during the inversion. The approaches are either deterministic or stochastic according to the mathematical apparatus.

─────────
✉Corresponding author.
   E-mail address: v.spichak@mail.ru (V.V. Spichak)
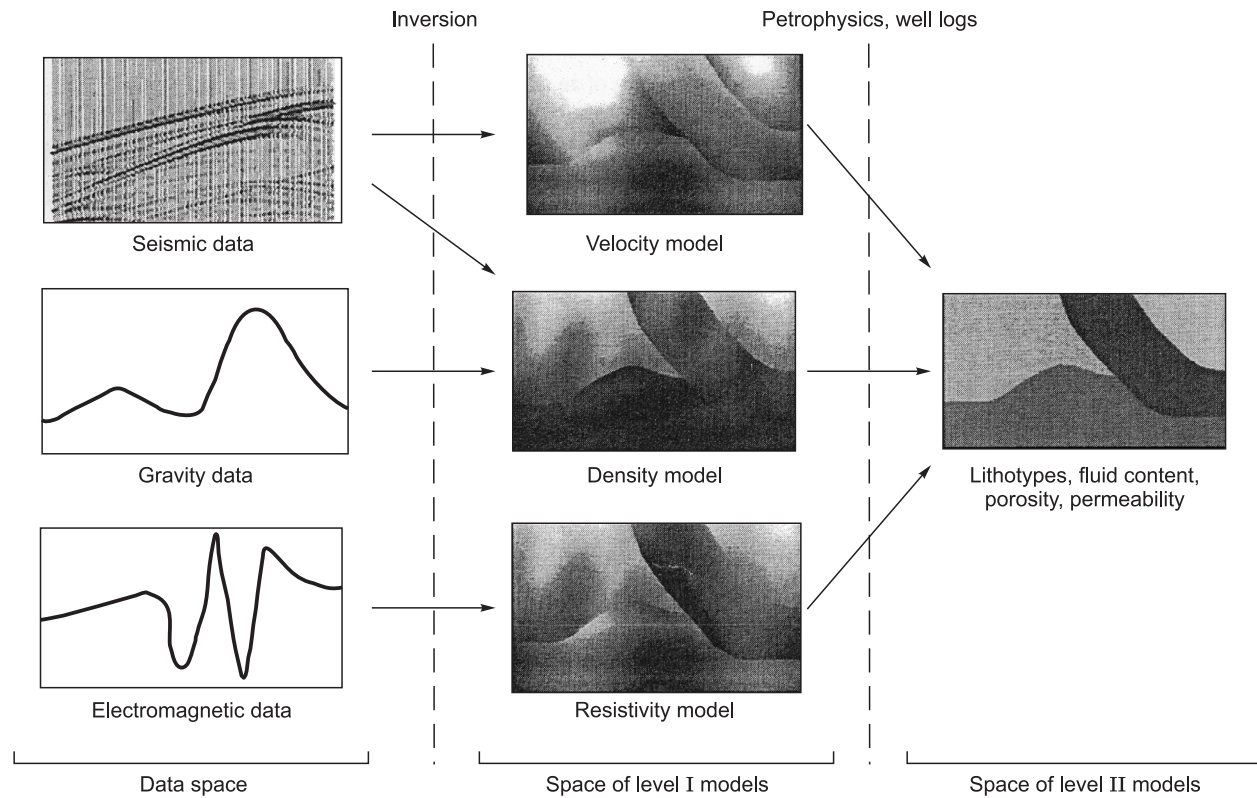
Fig. 1. Spaces of models and data in joint inversion of geophysical data, modified after (Bosch, 1999).

DETERMINISTIC APPROACH

The simplest way of joint inversion of all available data is optimization: designing an objective function that, once minimized, will provide a model that fits the best the observed data. The user can vary the influence of single data sets on the final result (level I parameters) by changing the respective weight coefficients (regularization term) in the functional (Lelievre et al., 2012). The approach can be implemented using modified Newton-Gauss iteration (Habashy and Abubakar, 2004), e.g., in petrophysical inversion (Abubakar et al., 2012; Gao et al., 2012). In the latter case, the parameters of level II (porosity and water content) are originally included into the minimized function assuming that they are related with level I parameters (conductivity, seismic velocity, and density) by empirical relationships. Joint inversion of electromagnetic and seismic data allows level II models of porosity and water saturation and leads to more accurate models than the separate inversion of single data sets (Abubakar et al., 2012; Gao et al., 2012). On the other hand, the exact effect of inversion for level II parameters compared with the two-stage procedure (level I and then II) remains unclear. The two-stage modeling does not require postulating empirical relationships between the parameters of different levels, which may distort the results.

In some cases, there are reasons to expect that the level I and II models are structurally similar and may fit a common geometrical model (Golizdra, 1978). Then, the curvature or gradients of physical properties characterize the geometrical features of the model and become prior linkage between two different data sets which is formalized and used compellingly in the inversion.

The structure operator of the model S can be found as (Haber and Oldenburg, 1997)

$$
S\,(\mathbf{m}) = \begin{cases} 0, & |\nabla^2\,\mathbf{m}|<\tau_1 \\ P_5\,(|\nabla^2\,\mathbf{m}|), & \tau_1<|\nabla^2\,\mathbf{m}|<\tau_2 \\ 1, & \tau_2<|\nabla^2\,\mathbf{m}| \end{cases} \tag{1}
$$

where $\mathbf{m}$ is the model parameter vector and P_5 is the fifth degree polynomial chosen such that S were a discontinuous twice differentiable function.

As follows from (1), the structural operator is always positive and normalized to the (0, 1) interval. Thereby (i) both positive and negative changes are taken into account in the same way and (ii) the operator S is invariant with respect to the scale of models. The application of such an operator is illustrated in Fig. 2 by two examples for $\tau_1 = \tau_2 = 10^{-5}$.

Correspondingly, the structural similarity requirement for two models is reduced to minimization of their difference, or the penalty function

$$
\varphi_1 = \sum_{i=1}^{N}\left[S(m_1^i) - S(m_2^i) \right]^2 \Rightarrow \min \tag{2}
$$
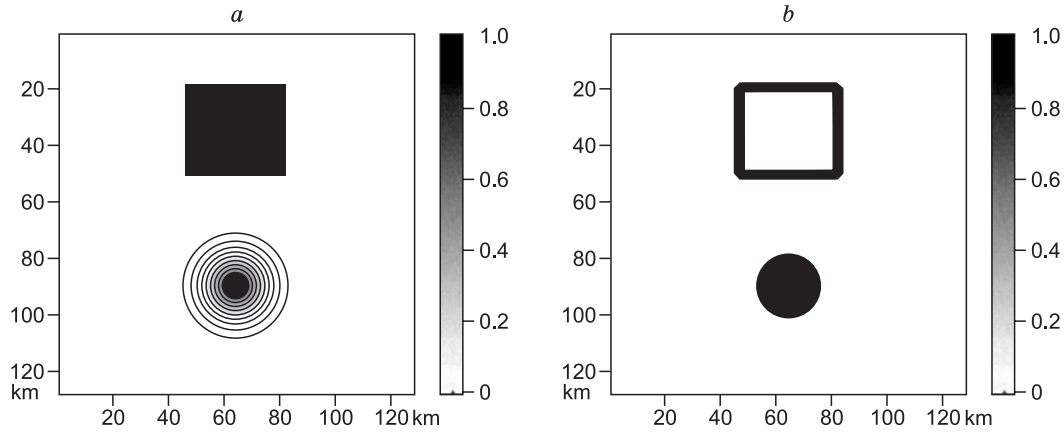
Fig. 2. The result of applying the structural operator: *a*, Models; *b*, images (at $\tau_1 = \tau_2 = 10^{-5}$) (Haber and Oldenburg, 1997).

where m_1^i and m_2^i are the values of model parameters in the *i*-th grid cell and *N* is the total number of cells, provided that the data are properly constrained.

The structural inversion has a pitfall that the arbitrary choice of the τ_1 and τ_2 thresholds of "large difference" may influence the solution: e.g., too small τ_1 and large τ_2 would mean that the structure covers the entire modeling domain. Another drawback is that the joint inversion neglects the direction of structure changes.

The problems were overcome by introducing a dimensionless function of cross-gradients (Gallardo and Meju, 2003) which, unlike the operator S (1), defines the geometrical similarity of two models as distribution of gradients rather than the values of parameters:

$$\varphi_2 = \sum_{i=1}^{N} \left[\nabla m_1^i \times \nabla m_2^i \right]^2 \Rightarrow \min \qquad (3)$$

To put it differently, the inversion uses structure constraints according to the parameter gradients. Note that zero

vector dot product in (3) may mean that the gradients are either perfectly collinear or zero at least in one model.

The approach of geometrical similarity between two models (Gallardo et al., 2005) is illustrated in Fig. 3, where the vectors in contour line maps (Fig. 3*a*, *b*) are parameter gradients in the respective model zones. Structural similarity is almost absent for vectors (1) and (2) which have large magnitudes but are directed almost orthogonally to each other but is present in the case of vectors (3) having opposite directions. The contour line map (Fig. 3*c*) shows that the highest positive or negative values of cross-gradients calculated for the models *p* and *q* fall within the zones of least structural semblance.

Gallardo and Meju (2007) applied the approach to joint inversion of magnetotelluric (MT) and seismic traveltime data (Fig. 4). The inversion was performed for synthetic electromagnetic and seismic data (Fig. 4*a*) that represent typical geological features, such as a sedimentary basin, undifferentiated crust, upper mantle, an isolated reservoir, a steep con-
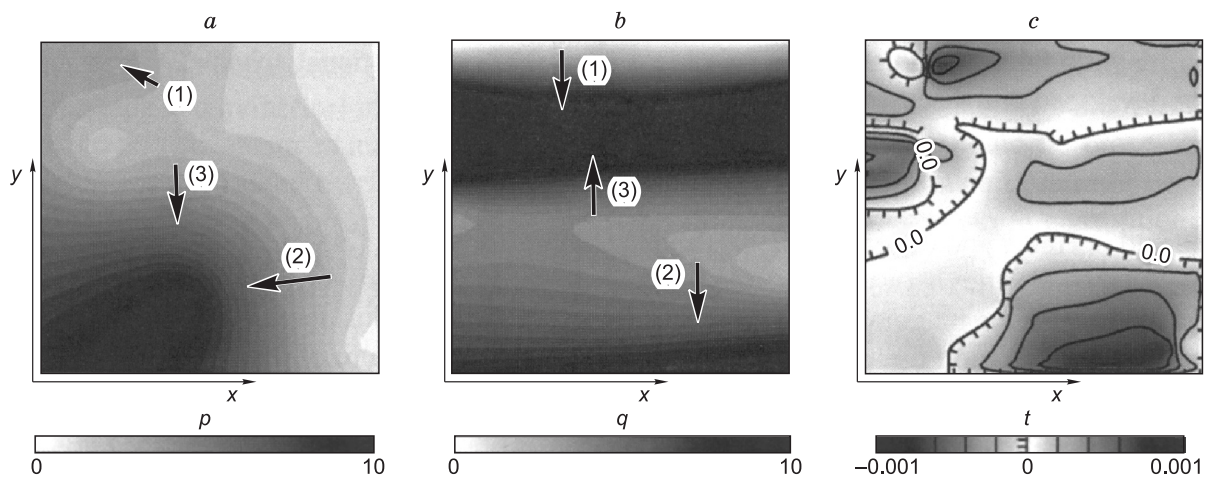
Fig. 3. Illustration of the concept of geometrical similarity between two images using schematic p (a) and q (b) images. The coincident vectors represent the gradients of the properties in corresponding zones. The contour map in panel *c* shows calculated values of the cross-gradient function for the *p* and *q* images (Gallardo et al., 2005).
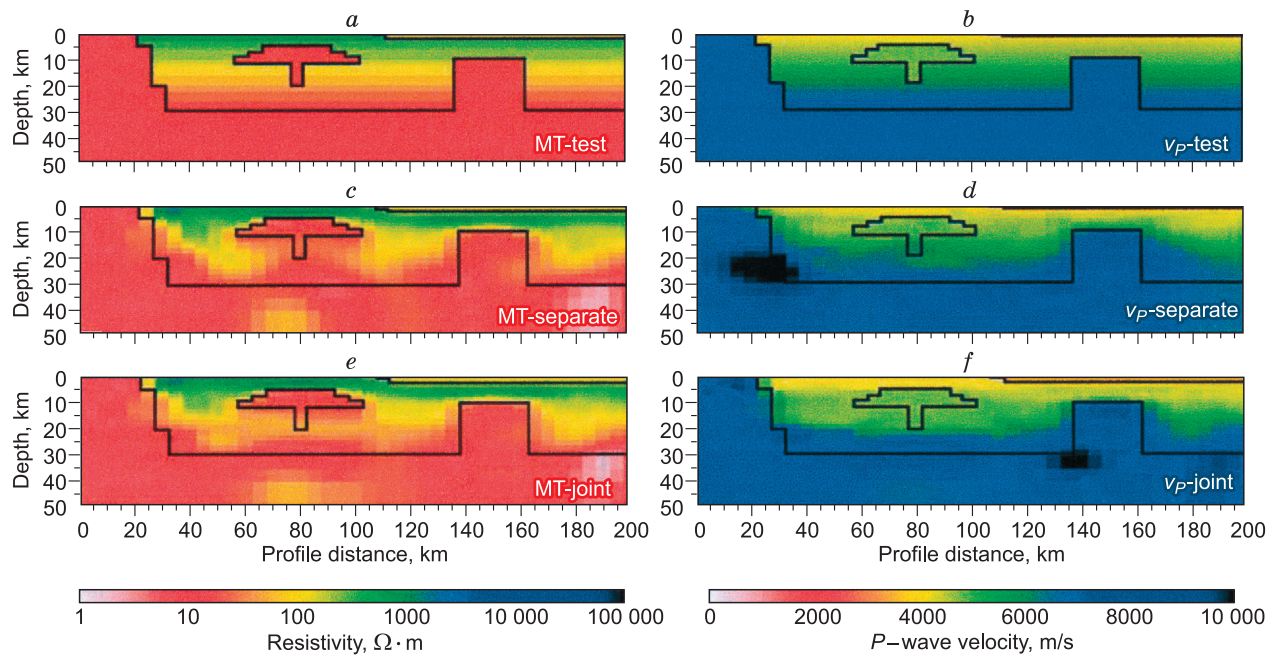
Fig. 4. Inversion of a single data set and joint cross-gradient inversion. *a*, *b*, MT-resistivity and seismic models, respectively; *c*, *d*, separate inversion of MT data and *P* arrivals, respectively; *e*, *f*, joint inversion of the same data sets. Thick lines outline test structures: sedimentary basin; crust; upper mantle; isolated reservoir; steep fault; and basement arch (Gallardo and Meju, 2007).

tact fault, and a basement arch. Joint inversion of two data sets (Fig. 4*e*, *f*), with added noise, provided better depth resolution than the separate inversion and better resolved the features beneath the isolated reservoir (Fig. 4*c*, *d*).

This inversion method has an ample literature (Haber and Oldenburg, 1997; Pinheiro et al., 1997; Kaipio et al., 1999; Gallardo and Meju, 2003, 2007; 2011; Gallardo et al., 2005; Saunders et al., 2005; Fregoso and Gallardo, 2009; Hu et al., 2009; Doetsch et al., 2010; Infante et al., 2010; Moorkamp et al., 2011; Hamdan et al., 2012; Lochbuhler et al., 2013), but its numerical implementation is often unstable and requires regularization. For this reason, Galardo et al. (2005) suggested applying joint inversion for simple structures only, which impairs the practical value of the method.

The regularization is run with a second-order tensor (covariance matrix), and the algorithm is implemented by quadratic programming which allows for simultaneous variations in the properties of two models (structural semblance); for this, Lagrangians are used without limiting the values of physical parameters which can be any real number and provide additional information to reduce the uncertainty of modeling results.

The main advantage of the structural approach is in posterior correlation of different physical properties (though the known correlation coefficient may be included *a priori* into the covariance matrix of the model). Yet, not necessarily the derived model would be useful and the petrophysical relationships would fit the true ones. Furthermore, the minimization of the cross-gradient function has to be checked carefully against petrophysical models and available local geology evidence.

The major drawback of the approach is that it requires structural semblance of the models. Note also that 3D inversion often consumes too much computer core memory and may be impossible, either with Lagrangians or with quadratic programming.

STOCHASTIC (MONTE CARLO) APPROACH

The approach consists in choosing an acceptable realization of a stochastic process among multiple generated versions. Processes with the same probabilistic parameters known from practice or theory (Sambridge and Mosegaard, 2002) can be simulated using Gibbs sampling (Geman and Geman, 1984), genetic (Holland, 1975; Haupt and Haupt, 2004; Moorkamp et al., 2006, 2007, 2010), or simulated annealing (Kirkpatrick et al., 1983; Cerny, 1985; Aarst and Korst, 1989; Bertsimas and Tsitsiklis, 1993; Harris and MacGregor, 2007; Mota and Monteiro Santos, 2010) algorithms.

The Bayesian approach, first applied by Goltsman and Kalinina (1973) in Russia for integration of geophysical data, appears to be most flexible and allows appropriate modeling by combining the collected data with geological and geophysical priors. The approach was developed in many later studies (Tarantola, 1987; Backus, 1988; Mosegaard and Tarantola, 1995; Bosch, 1999; Bosch et al., 2001; Press, 2002; Muñoz et al., 2010; Dell'Aversana et al., 2011; Tondi et al., 2012; JafarGandomi and Binley, 2013; Jardani et al., 2013; MacCalman et al., 2014; Mellors et al., 2014; Ren et al., 2017). The approach of this kind suggested by Bosch (1999) for joint inversion of geophysical, petrophysical, and geostatistical data, constrained by prior geological

evidence, uses statistical descriptions of the model structure at the input and yields separate models explicitly related with geophysical data (via a physical theory) and lithological (or other) models.

Assume that $\mathbf{m} = \{m_1, m_2, \ldots, m_N\}$ is a set of all level I or II parameters; M is the respective set of all model parameters ($\mathbf{m} \in M$); $\mathbf{m}_p$ is the vector of level I model parameters ($\mathbf{m}_p \in M_p$, where $p = 1, \ldots, k$); and $\mathbf{m}_s$ is the vector of level II model parameters ($\mathbf{m}_s \in M_s$ where $s = k + 1, \ldots, N$); correspondingly, $M = M_p \times M_s$.

The information on the properties of the subsurface and their distribution can be expressed via the probability density function (pdf) defined over a set of model parameters. Bosch et al. (2001) inverted multidisciplinary geophysical data constrained by geological and geostatistical priors. They used data on lithology, statistical correlation between lithology and rock physics, and a joint likelihood function defined on the sets of individual model parameters. The Bayesian inversion leads to the posterior pdf

$$p_{apost}\,(\mathbf{m}_s \mid \mathbf{m}_p) = c\,\theta_{s/p}\,(\mathbf{m}_s \mid \mathbf{m}_p)\,p_{apr}(\mathbf{m}_p)\,L\,(\mathbf{m}_s). \qquad (4)$$

Each term in (4) represents different components of the information:

– pdf function $p_{apr}(\mathbf{m}_p)$ defined over the primary model parameter space describing prior information on lithology;

– conditional probability $\theta_{s/p}(\mathbf{m}_s|\mathbf{m}_p)$ describing information on the secondary model parameters, their spatial relationships, cross relationships, and dependence on the primary properties;

– joint likelihood function $L\,(\mathbf{m}_s)$, which measures probability misfit between the data calculated from the joint model and the geophysical observations;

– normalization constant c calculated based on the probabilistic postulate that an inverse solution exists over the set of all parameters (M).

Thus, the resulting pdf $p_{apost}\,(\mathbf{m}_s|\mathbf{m}_p)$ consists of two factors corresponding to two different information sources: joint likelihood function $L(\mathbf{m}_s)$, which is a dot product of independent likelihood functions associated with each geophysical data set and joint prior pdf. The latter, in turn, comprises the marginal $p_{apr}\,(\mathbf{m}_p)$ and conditional $\theta_{s/p}\,(\mathbf{m}_s|\mathbf{m}_p)$ pdfs in the primary (physical) and secondary (lithological) spaces of model parameters.

The conditional pdf $\theta_{s/p}\,(\mathbf{m}_s|\mathbf{m}_p)$ can well account for empirical or theoretical petrophysical laws relating different properties of rocks. The rock physics, obviously controlled by lithology, is a macroscopic expression of rock structure (composition, texture, and genesis). This relationship was studied for different types of subsurface and can be investigated empirically for each specific area.

The marginal pdf $p_{apr}\,(\mathbf{m}_p)$ is good to describe the properties that are better constrained by priors based on the knowledge of local geology (geological maps, probable lithofacies and their geometrical relationships, stratigraphy, etc.).

The statistical relationships between properties within each lithology (e.g., average values and variograms or, more

generally marginal and conditional pdf) can be better described and may be uniform at favorable conditions. This assumption is of special importance because most of models used for estimation and modeling of the Earth properties assume that the data are statistically homogeneous or spatially stable. If the properties are assumed to be uniform within each lithofacies, the conditional pdf will be trivial and the inversion will consist in estimating primary model parameters. Specifically, the joint pdf for a single property of a geophysical data set becomes reduced to a simple posterior pdf for inversion of independent data sets, e.g., the Bayesian inversion of electromagnetic data (Roussignol et al., 1993; Grandis, 1994; Spichak, 2005; Spichak et al., 1999).

As mentioned above, level I models may include also other properties (porosity, permeability, saturation, etc.) according to the problem formulation. The key primary properties of the subsurface depend on the problem scale and type: lithology for shallow crust; lithology, porosity, fluid saturation, and stratigraphy for basins; etc. Generally speaking, the level I parameters should be useful for the identification and characterization of lithofacies and govern statistically dependent level II parameters.

Since all functions in (4) are complex, the posterior marginal pdf for the model parameters is not closed and can be calculated only numerically with statistical methods (their description is beyond this publication). The posterior values of levels I and II are easily found after the function has been
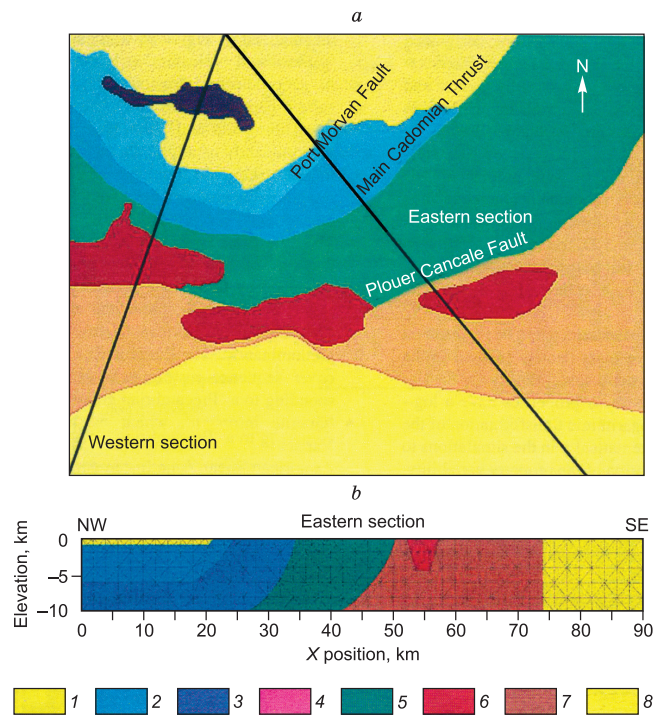
Fig. 5. Plan view (*a*) and cross-sections (*b*) of a preliminary 3D model along a profile (NW—SE) of panel *a* (Bosch et al., 2001).
1, sediments, *2*, volcanics, *3*, gabbro, *4*, gabbrodioritic intrusion, *5*, migmatite, *6*, granitic intrusion, *7*, Precambrian continental margin, *8*, Precambrian continent.
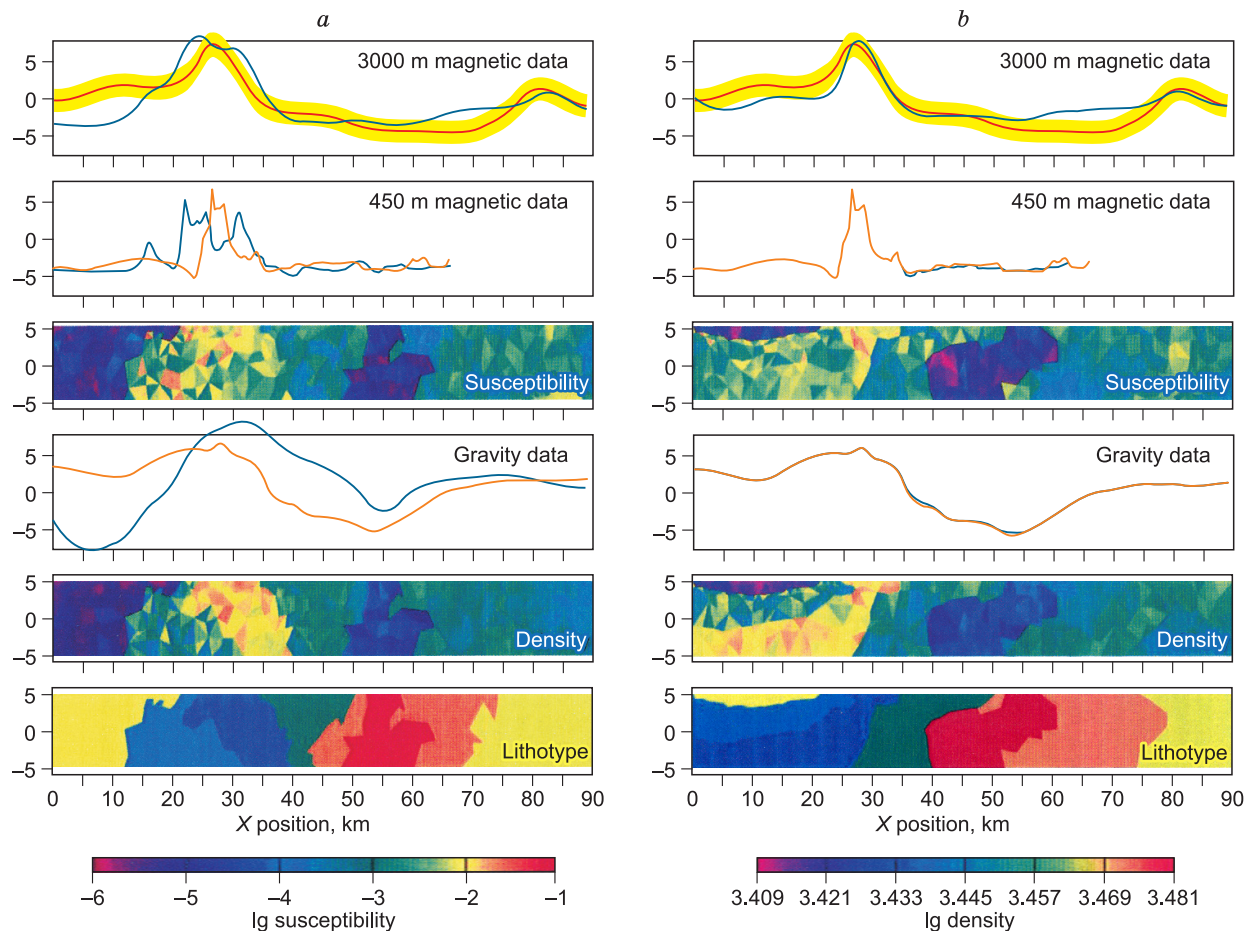
Fig. 6. Prior (*a*) and posterior (*b*) models resulting from Bayesian joint inversion of magnetic and gravity data (geological model along profile NW-SE from Fig. 5), modified after Bosch et al. (2001).
The density and magnetic susceptibility scales (bottom) are logarithmic; lithotypes are described in Fig. 5. Observed and calculated data are in red and blue, respectively. Yellow belt indicates +/-1 standard deviation uncertainty in the observed data.

determined using multiple joint models chosen during the Bayesian inversion.

The steps of joint inversion of magnetic and gravity data to obtain lithological sections (Bosch et al., 2001) are shown in Figs. 5 and 6: map of local geology (Fig. 5*a*) and preliminary lithological cross-sections in the NW-SE and NE-SW directions (Fig. 5*b*), and joint inversion of magnetic and gravity data to posterior lithological patterns, as well as joint magnetic susceptibility and density patterns, with reference to geological and geophysical priors (Fig. 6).

Thus, the stochastic techniques can provide formalized tools for including geological and geophysical priors and peer inspection results for integration of different geophysical data sets, which is advantageous over the deterministic approach. Furthermore, the inversion not only yields the sought parameter distributions but also allows posterior evaluation of uncertainty at each grid node. On the other hand, the inversion quality depends on whether the parameters of random processes in the algorithms faithfully represent the reality. The approach may be problematic because it

requires specifying prior pdf in all parameters, which are assumed to have a Gaussian distribution. Furthermore, the computation consumes extremely large computer memory and time resources and may take many weeks, even with advanced multi-processor systems.

SEQUENTIAL INVERSION

Instead of inverting independent data sets jointly, inversion can be interactive and sequential: the inversion results for one data set can be used as starting models to invert other data. The approach was first suggested by Lines et al. (1988) and was revisited in the 2000s (Dell'Aversana, 2001, 2006, 2014; Dell'Aversana et al., 2002, 2011; Zhu and Harris, 2011; Paasche et al., 2012). It can be better understood with the example of MT and gravity data inverted in a series of sequential steps, as in (Dell'Aversana, 2001):

(1) building a detailed velocity model following a tomographic inversion of the first breaks (Fig. 7);
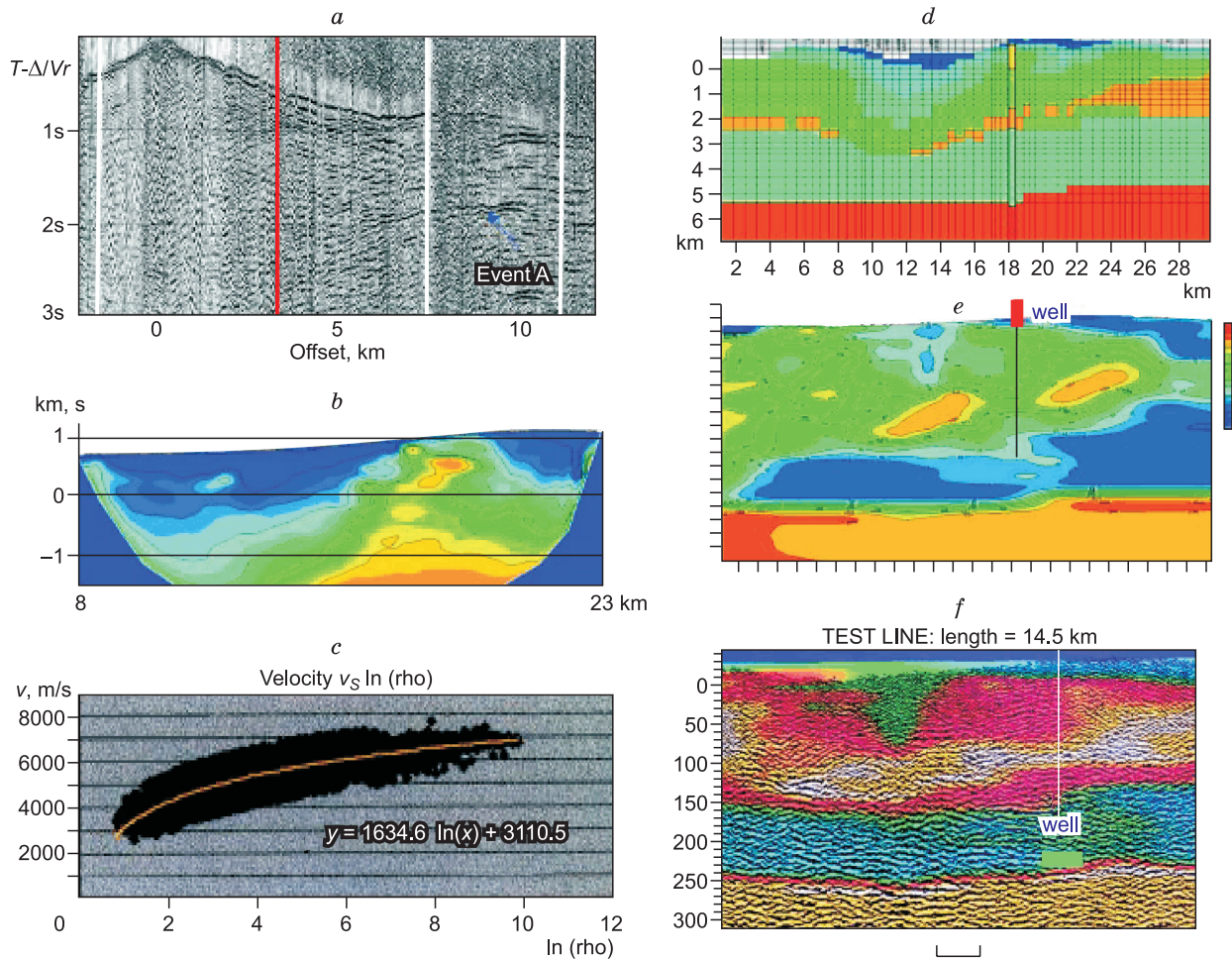
Fig. 7. Steps of interactive inversion, modified from (Dell'Aversana, 2001): *a,* Common receiver gather (seismic section); *b,* tomographic v_P model; *c,* empirical relationship between resistivity and velocity, from well log analysis; *d,* resistivity model derived from seismic tomography and borehole information; *e,* final magnetotelluric model; *f,* parametric model imported into the seismic section.

(2) transforming the velocity/depth section v_P into a resistivity/depth section R, with reference to resistivity well logs analyzed for possible empirical velocity-resistivity relationship. The best fit curve in the velocity/resistivity cross-plot (Fig. 7*c*) has the analytic form

$$v_P = a(\ln(\ln(R))) + b, \tag{5}$$

which is used to convert velocity from the model of (Fig. 7*b*) to resistivity (Fig. 7*d*);

(3) forward MT modeling using the derived resistivity model as a starting one; separating the model into the TE and TM modes; correcting static shift problems;

(4) a series of 2D MT inversions using the synthetic resistivity section of step 3 as a reference model and the resistivity measured in boreholes as constraints (see Fig. 7*e*) for the final model;

(5) checking the quality of the resistivity model (Fig. 7*e*) by modeling the gravity. For this the resistivity section is converted to density according to the empirical equation derived from well logs and geological hypotheses. Although the gravity inversion is not unique in principle, it can constrain the range of geometry and density variations and thus reduce the ambiguity;

(6) converting the resistivity model (Fig. 7*e*) back to a new velocity section, using the same empirical formula (5), with subsequent depth-to-time conversion (Fig. 7*f*).

If necessary, the new seismic section is further used to simulate resistivity, etc. The interactive cycle 1-6 continues until the inversion errors become stable for all types of data; eventually it yields an integrated multidisciplinary geophysical model, which is easier to interpret than the initial model (compare Figs. 7*a,f*).

The approach is advantageous in being relatively simple and requiring much less computer core memory than the simultaneous joint inversion. On the other hand, the interactive process uses relationships between the prior petrophysical properties measured in boreholes or in cores. Yet, these empirical relationships may be not always available, and not necessarily valid throughout a 2D or especially 3D model.

CLASSIFICATION METHODS

A basically different approach to integration of geophysical data consists in separate inversion of different data sets (level I models) followed by detection of regions with homogeneous physical properties using classification methods; the homogeneous regions are used to predict level II parameters with reference to expertise and geological and geophysical priors. The approach stems from the basic assumption that geological objects differ in their physical properties and are detectable by individual measurements of the respective parameters. Thus, the structures are detectable if their difference in the space of parameters exceeds the variance of parameters within their limits.

This section focuses on main approaches to joint analysis of separate inversion results for single data sets, without going into details of each inversion procedure. The most frequently used classification methods (Reimann et al., 2008), such as cluster analysis, Gaussian classification, k-means clustering, and discriminant analysis, are characterized briefly below.

• *Cluster analysis* is grouping according to proximity of samples in the space of properties. Unlike other classification methods that use training samples for statistical modeling, grouping in cluster analysis is based on properties without regard to lithology (Hartigan, 1975; Kaufman and Rousseeuw, 2005).

• *Gaussian classifier* is based on the assumption that the vector of properties has an *n*-dimensional Gaussian distribution of the conditional pdf within each lithological group. Each lithofacies should have its center and covariance matrix determined from training samples (Rasmussen and Williams, 2006).

• *K-means clustering* implies iterative search of a set of points (centers) so as to minimize the mean squared distance from each data point to its nearest center in training samples
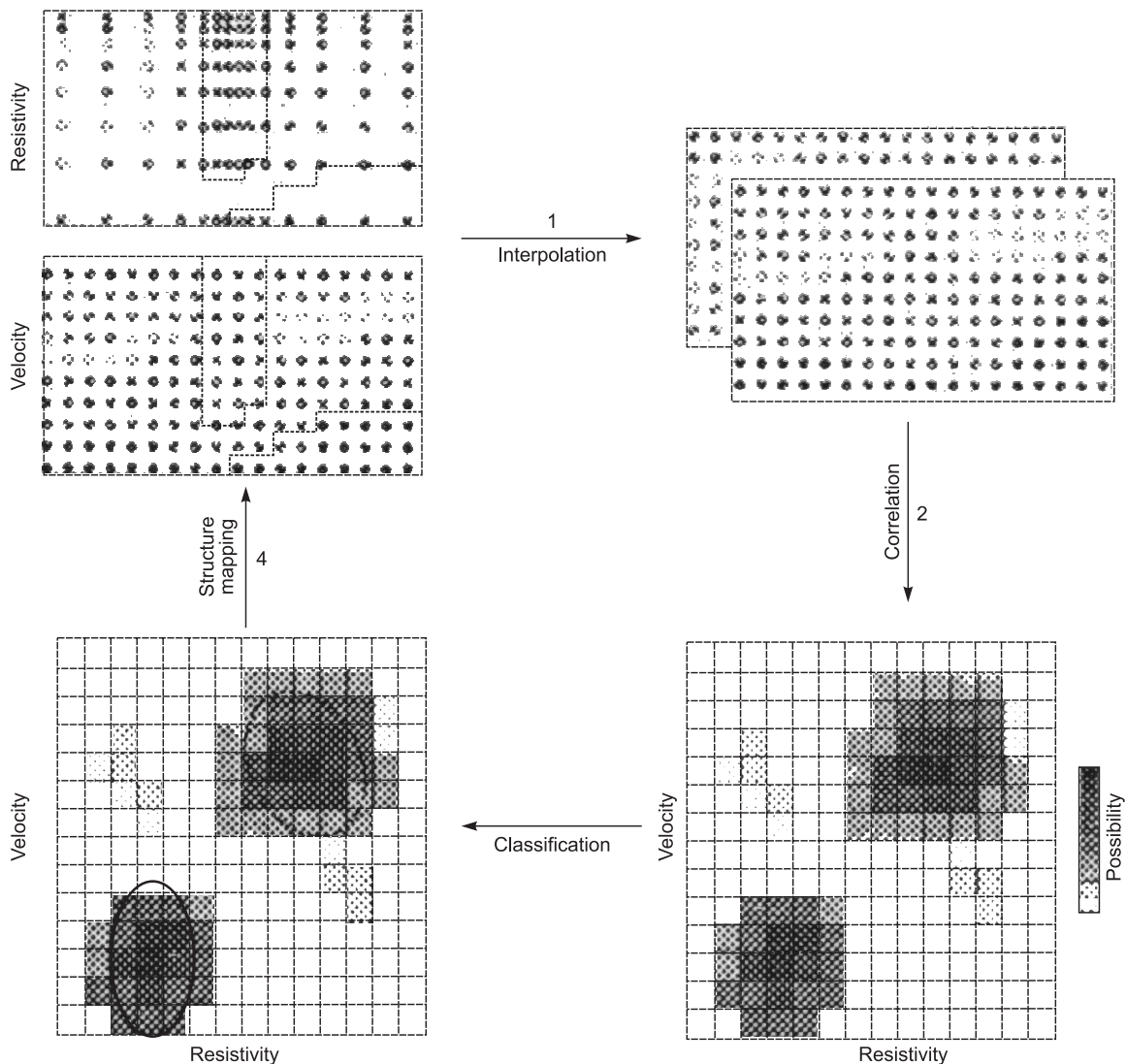
Fig. 8. Statistical structural classification using level I models (Bedrosian, 2007).
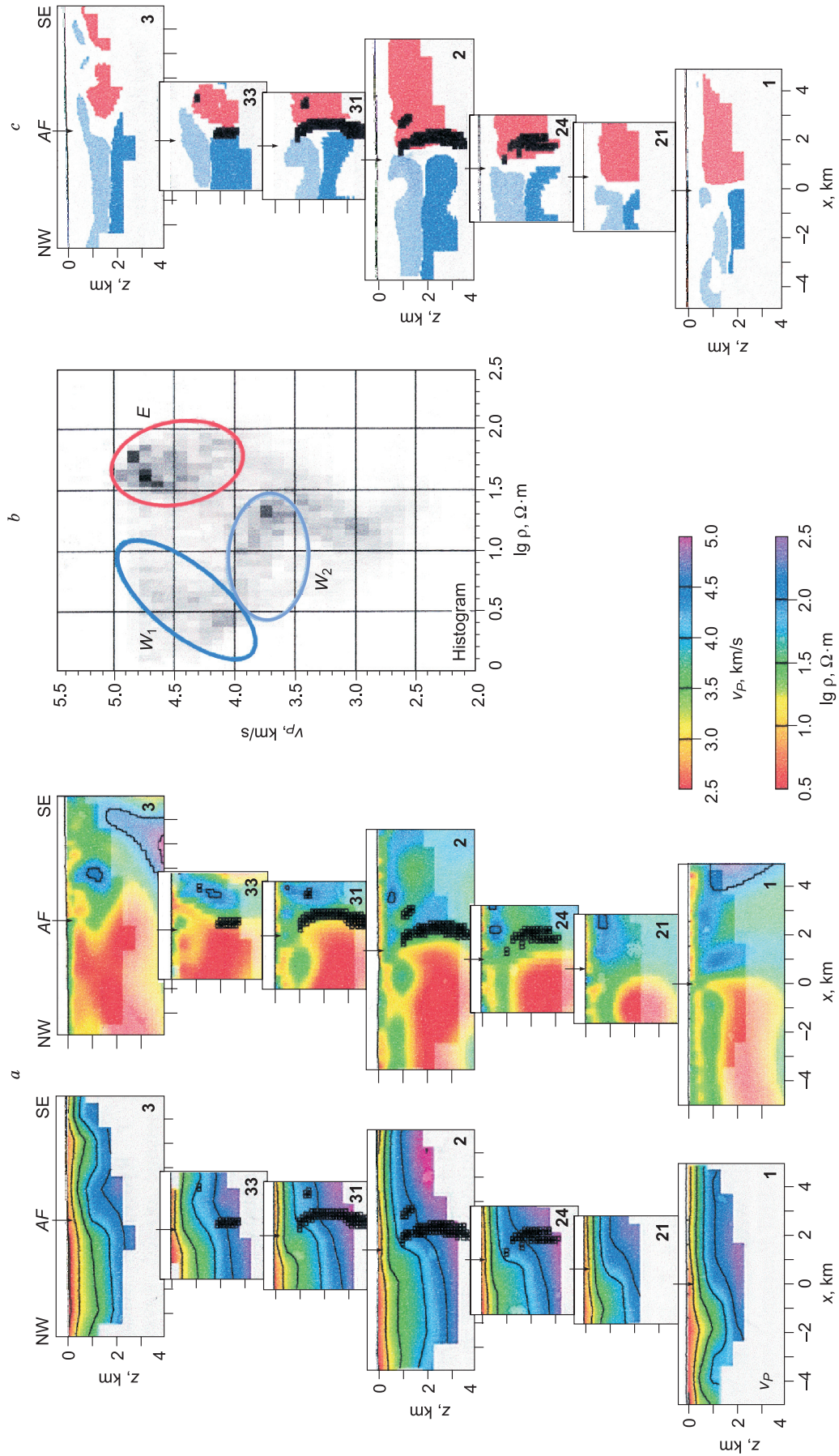
Fig. 9. Geophysical subsurface structure around the Arava Fault (arrows indicate the surface trace of the fault, AF).

a, Slices through the 3-D P velocity model v_P (left) and 2-D electrical resistivity models log ρ (right); *b*, histogram of vp *vs.* log r. Good correlation is in black; ellipses outline clusters; *c*, data pairs (pixels) from the outlined regions in the histogram remapped into the subsurface (dark blue, light blue, and red colors correspond to clusters W_1, W_2, and E, respectively); Arabic numerals denote profile numbers (Maercklin et al., 2005).

(Kanungo et al., 2002). Each point is assigned to one of k clusters; thus the center represents each cluster while each point is closer to the center of its cluster than to the centers of other clusters.

• *Discriminant analysis* searches the functions of properties which separate groups in an optimal way (in terms of root mean square) in order to choose the combination of linear coefficients to maximize the variance of group centroids while minimizing the variance within the groups (Huberty, 1994). The discriminant functions are used as additional coordinates for data presentation: a discriminant space. This method has widespread applications of the graphic representation of multidimensional data and classification.

Cluster analysis is most often performed by probabilistic or neural network methods.

Probabilistic clustering requires interpolating (Fig. 8) the parameters obtained by inversion of independent data sets to the common coordinate grid (Bedrosian, 2007), assuming that each level I model is specified by discrete points at its coordinate grid nodes so that each node has its set of points for two or more physical parameters. Then joint pdf is determined in the common space of parameters (correlation) and is used as a basis for detecting local zones of high probability density, i.e., identifying classes and their boundaries in the common space of parameters (classification). At the final step (mapping), these zones are mapped back to the coordinate space in which each class determines the geological structure (lithology).

Figure 9 illustrates the use of this approach with an example from (Maercklin et al., 2005). It shows 2D slices of the 3D velocity structure v_P (left) and logarithmic resistivity log r (right) derived by separate inversion of seismic and MT data sets, respectively (Fig. 9*a*), from the vicinities of the Arava fault (*AF*). The jointly analyzed level I models are presented as a histogram of velocities v_P versus resistivities log r (Fig. 9*b*), with darker regions corresponding to stronger correlation and ellipses outlining clusters of best correlated parameters. Finally, the outlined clusters (Fig. 9*c*) are mapped back from the space of parameters to that of coordinates.

Bedrosian et al. (2007) used an approach based on Gaussian clustering assuming that lithotypes are spatially connected domains characterized by uniform physical properties which are normally distributed about a mean. The optimum number of classes (clusters) was determined from examination of global misfit as a function of the number of fit classes.

In other publications (Muñoz et al., 2010; Jousset et al., 2011), the clusters were related to geological structures based on regional stratigraphy and on measured velocity and resistivity values, with reference to geological surveys, well logs, and independent geophysical data. Correlation of independent models showed that no simple empirical relationships existed between different physical properties, except for local correlations, each corresponding to a separate lithology.

Neural classification techniques, such as maximum correlation similitude (Spichak et al., 2006, 2007) or self-orga-
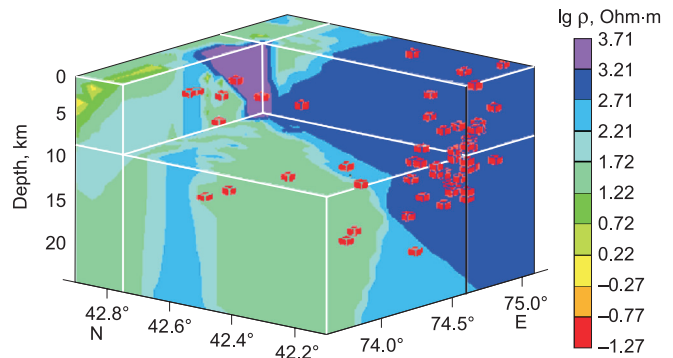
Fig. 10. 3D resistivity model of the northern Tien Shan crustal area. Elementary prisms (red) are zones of best correlation between resistivity and density of earthquakes (Spichak et al., 2006).

nizing maps (Kohonen, 2001) are based on learning of neural networks by correspondence between physical parameters.

The *maximum correlation similitude* technique, like the probabilistic methods, requires interpolation of level I models onto a common grid followed by search of best correlation regions for the target physical properties (Spichak et al., 2007). The clusters can be considered as spatially stable regions and taken for reference in further lithological division. The approach can be used to reveal potentially active seismic areas (Fig. 10) by joint analysis of resistivity and earthquake density patterns. Zones of maximum correlation (elementary prisms) correspond to resistive brittle crust and deep faults.

This approach to integration of geophysical data is advantageous over probabilistic clustering (Maercklin et al., 2005; Bedrosian, 2007; Bedrosian et al., 2007). Namely, (i) it provides better accuracy due to neural interpolation for estimating two physical parameters at the same grid nodes instead of the conventional kriging; (ii) classification in the coordinate space without interpolation to the space of parameters and back (Fig. 8) allows avoiding side problems (e.g., assuming a Gaussian distribution of parameters, which is not always the case); (iii) the optimal number of clusters is set automatically rather than being specified by the user. On the other hand, the method is limited to only two simultaneously analyzed properties.

The technique of *self-organizing maps (SOM)* uses unsupervised learning by the Kohonen rule (Kohonen, 2001) with reference to *a priori* information on the number of clusters with similar properties, which are outlined in the target space (Bauer et al., 2012). The Kohonen network consists of two layers (Fig. 11), and each neuron of the first (input) layer is connected with all neurons of the second (output) layer arranged in a 2D grid (map). The neurons of the input layer correspond to physical properties of rocks (seismic velocity v_P, velocity anisotropy, and attenuation in our case); the number of output neurons (cluster elements) is specified externally and defines the maximum possible
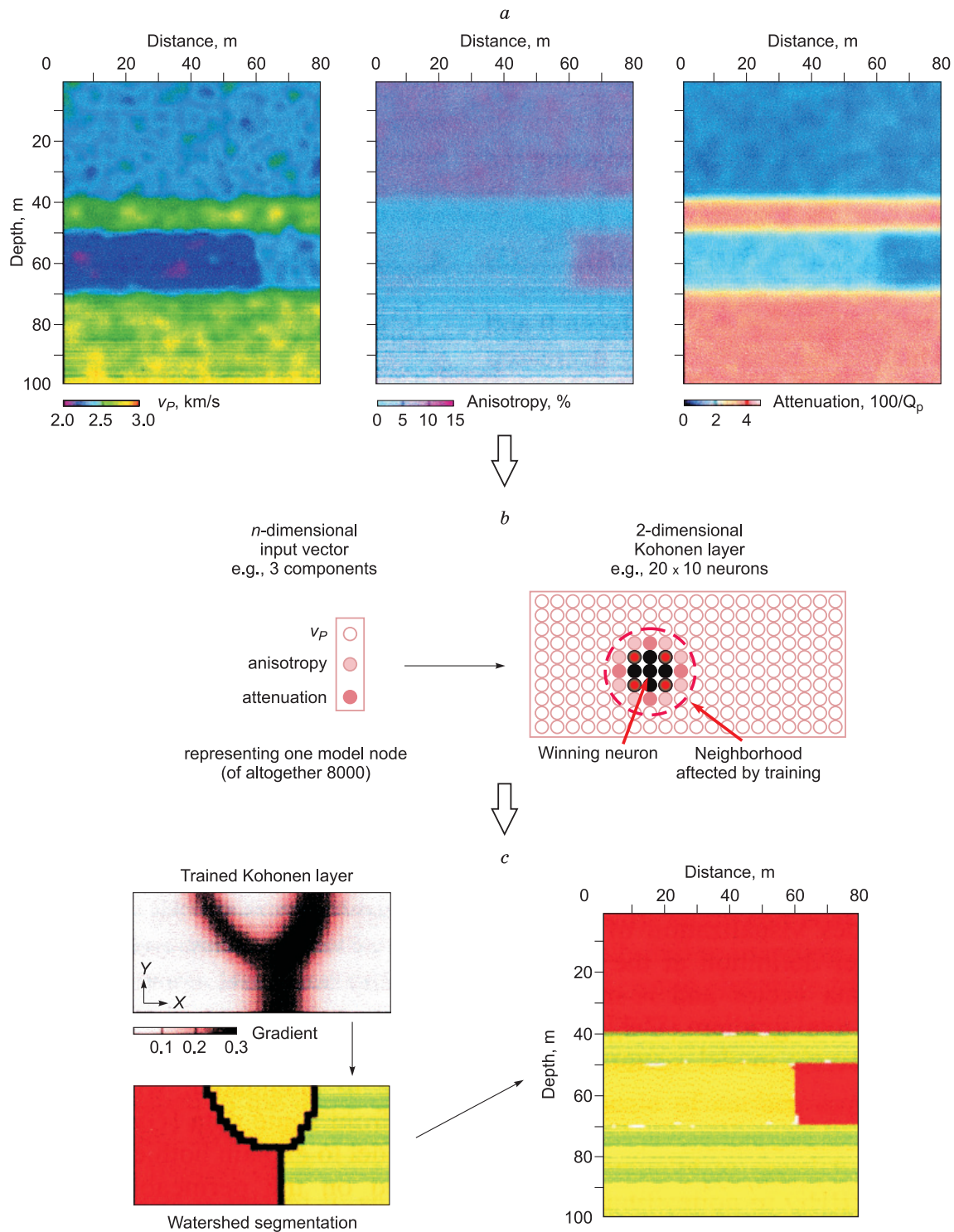
Fig. 11. Use of SOM technique for joint interpretation of level I models: *a*, Synthetic models (from left to right: *P* velocity v_P; velocity anisotropy; attenuation); *b*, Kohonen learning; *c,* classification (map) (Bauer et al., 2008).

number of clusters distinguishable in the input data (e.g., lithotypes).

In the Kohonen approach, the output neurons are not matched to reference values (unlike the error back-propagation technique). The neural network learns from input train-ing samples, which are physical parameter values (points at gird nodes). The learning is competitive: the neurons of the cluster layer that represents superparameters compete with one another on a winner-takes-all basis, and the winner is the neuron whose weight vector is most similar to the input

(a three-component vector in our case); each input vector in this process belongs to some cluster element.

Once the learning has been completed, the network can classify the input examples into groups of similar elements. The neurons in the output layer faithfully simulate the pattern of training samples in the multidimensional space of parameters. Thus, the Kohonen self-organizing maps provide mapping of the multidimensional space of parameters into that of clusters (Spichak et al., 2015).

The above approach was applied previously (Spichak et al., 2008) to obtain a cluster petrophysical cross section from three components corresponding to different physical properties: seismic velocity, effective density, and resistivity along a fragment of the regional transect 1-SB in East Siberia. The fragment between 400 and 600 km along the transect is located within the Yenisei Foredeep, the Kamo Arch, and the western Baikit Uplift (Fig. 12). The transect traverses two gas fields (Omorinsky between 500 and 520 km and Yurubchen-Takhoma at 540—580 km); the depth intervals of low density in the crust correspond to gas reservoirs.

Panels *a* and *b* in Fig. 12 show, respectively, a SOM petrophysical cross section and physical properties within individual clusters. The gas fields are marked by petrophysical anomalies (clusters 1—4), with small vertical channels at
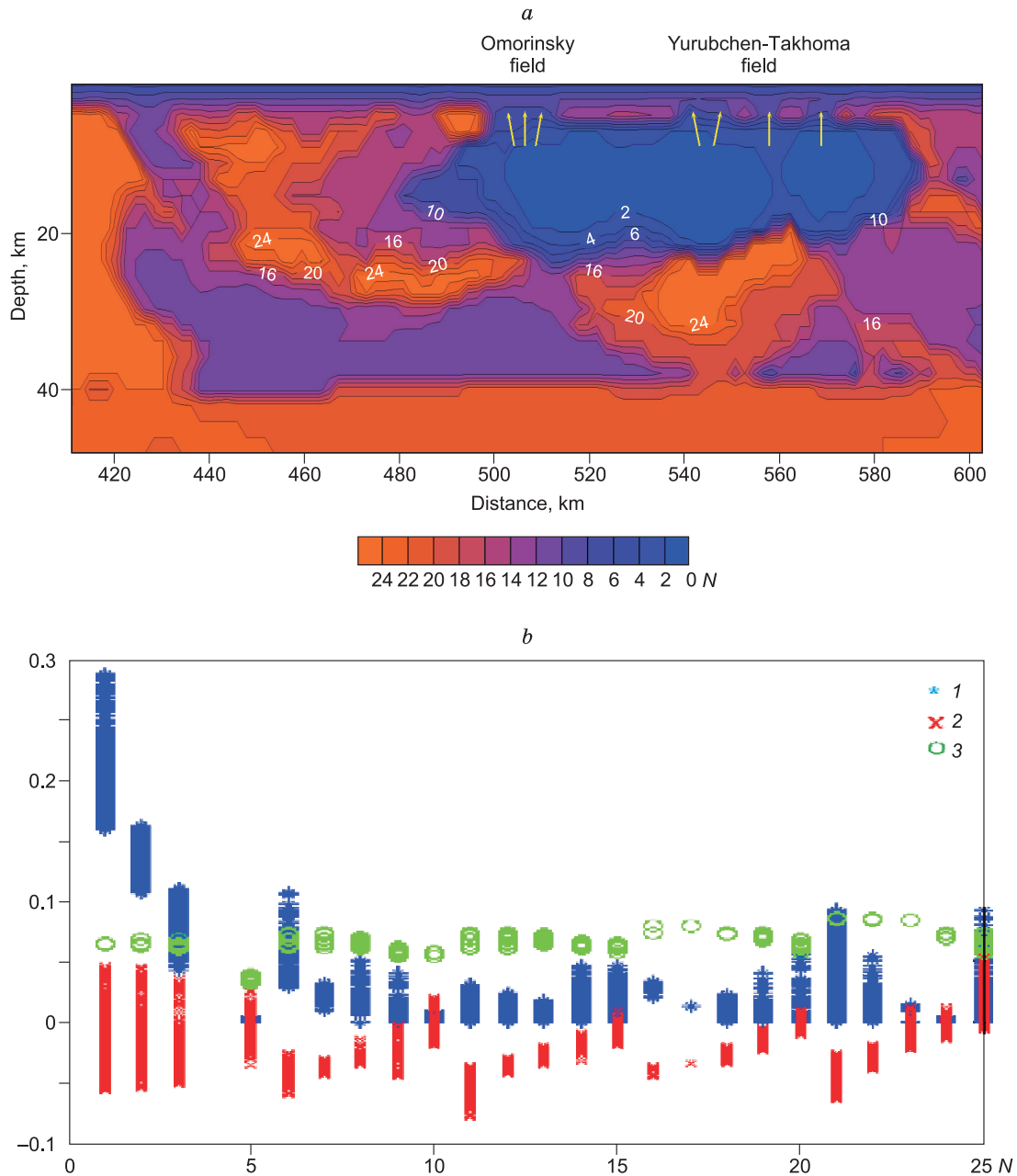
Fig. 12. Cluster petrophysical cross-section along profile 1-SB. *a,* Cluster section, *b*: petrophysical clusters (Spichak et al., 2008). 1, resistivity, $\times 10^5$ Ohm·m; 2, effective density, g/cm^3; 3, P velocity, $\times 10^5$ m/s.
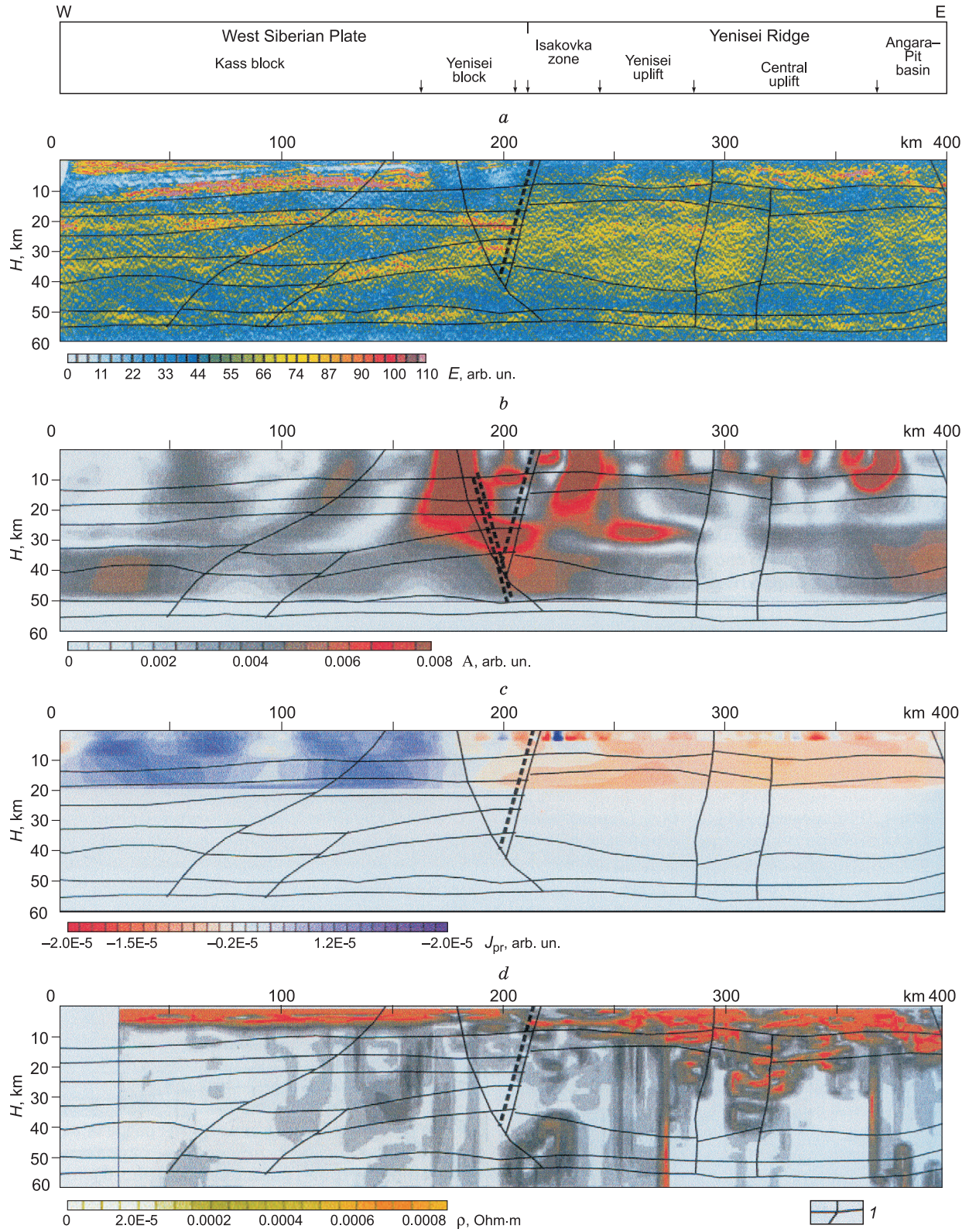
Fig. 13. Generalized geometrical model of the crust along transect 1-Siberia, compared with models derived from independent data sets. *a*, Seismic energy cross-section, *b*, parameter α for effective density, *c,* parameter α for effective magnetization, *d,* parameter α for resistivity (Kaplan et al., 2006). *1*, layers and blocks in the generalized geometrical model.

shallow depths, possibly, gas conduits (Fig. 12, *a*). The presence of such anomalies in the vicinity of hydrocarbon accumulations may be a necessary (but not always sufficient) indicator of petroleum potential.

HYBRID APPROACHES

The construction of a cluster cross-section may be preceded by general geometric modeling of the subsurface, by different techniques: cross-gradients (Hellman et al., 2017) or localization of high-gradient zones in models based on independent data sets (Nikitin et al., 2003; Cheremisina et al., 2006; Kaplan et al., 2006; Galuev and Kaplan, 2009). The cited authors used the so-called differential-normalized parameter (α) to better highlight the properties of the subsurface and to proceed to dimensionless units. The parameter α is a depthward increment (total differential in the general case) of logarithmic seismic impedance (density, magnetization, or resistivity):

$$\alpha = 1/2 \; d/dz \ln P \, dz, \tag{6}$$

where *P* stands for $v \cdot \varsigma$ (*v* is seismic velocity and ς is density) for seismic, ς (density) for gravity, and ρ (resistivity) for resistivity data.

Since α (6) represents relative heterogeneity of the subsurface, its extreme values traceable in the section may delineate interfaces between blocks with homogeneous physical properties. Such an integrated crust model along a

fragment of the 1-SB transect is compared with models based on independent data sets in Fig. 13 (Kaplan et al., 2006). The next step consists in estimating the statistics of each property within the blocks (using the K-means technique) and geological modeling from block-average physical properties. Finally, each set of properties within a block is related to a level I model parameter, most often a lithotype (Fig. 14).

This approach is advantageous as the boundaries of physically homogeneous blocks are traceable in contour line maps of extreme α values which limit the zones of smooth changes. Geometrized modeling with subsequent determination of physical properties in the respective homogeneous blocks becomes possible when the block boundaries coincide in different level I models.

The disadvantage of the approach is a reverse side of its advantage, as it often happens: the final model may be poorly reliable in the case of mismatching boundaries of homogeneous blocks corresponding to different physical properties. Like in the method of cross-gradients (see above), if the hypothesis does not fit reality, the general structure and its population are far from reality as well.

The discussed clustering techniques are based uniquely on statistical correlation of physical properties in the general space of parameters and remain independent of theoretical or empirical linkage between the physical properties of rocks. These methods can be also useful for multi-dimensional statistical description of relations between rock properties and lithology, as well as for the choice of properties
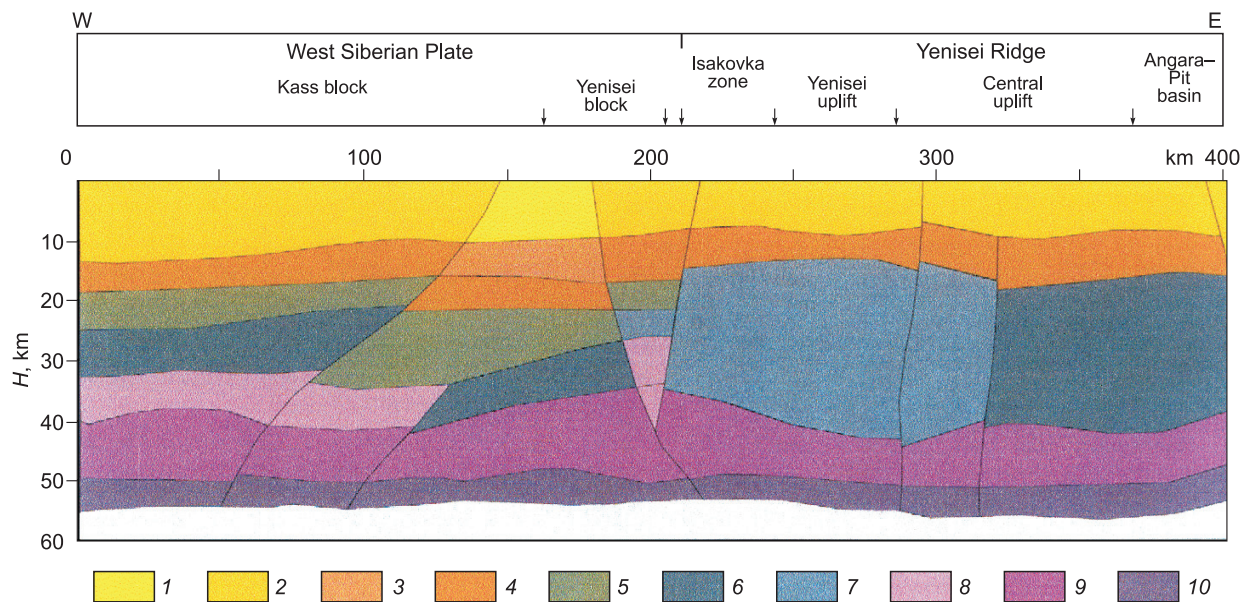
Fig. 14. Predicted lithology distribution along transect 1-SB (Kaplan et al., 2006). *1*, $\sigma = 2.63$ g/cm³, $v = 5800$ m/s, clastic-carbonate sediments; *2*, $\sigma = 2.64$–2.7 g/cm³, $v = 5600$–6100 m/s, carbonate-clastic sediments; *3*, $\sigma = 2.67$–2.70 g/cm³, $v = 6500$ m/s, gneisses, schists, felsic igneous rocks; *4*, $\sigma = 2.71$—2.73 g/cm³, $v = 6700$–7100 m/s, quartz-biotite two-mica schists, intermediate igneous rocks (granodiorite, diorite, monzonite); *5*, $\sigma = 2.80$—2.82 g/cm³, $v = 6500$–7100 m/s, biotite-hornblende and amphibole schists, crystalline gneisses and intermediate igneous rocks; *6*, $\sigma = 2.85$–2.89 g/cm³, $v = 7300$–7500 m/s, gabbro, gabbro-diabase and amphibolite; *7*, $\sigma = 2.85$–2.89 g/cm³, $v = 6800$–7100 m/s, gabbro, gabbro-diabase and amphibolite (possibly, highly fractured); *8*, $\sigma = 2.93$–2.98 g/cm³, $v = 7600$–7800 m/s, gabbro, basalt, schists and hornblende schists; *9*, $\sigma = 3.0$ g/cm³, $v = 7900$–8300 m/s, dunite, peridotite, pyroxenite, etc.; *10* – $\sigma = 3.07$ g/cm³, $v = 8300$ m/s, eclogite, etc.

and geophysical data suitable for lithology prediction in specific exploration scenarios. In terms of methodology, the approach highlights the structural conformity of models and provides natural tools for regularization of joint inversion.

CONCLUSIONS

The choice of geophysical data used for joint inversion depends on problem formulation in terms of superparameters (e.g., lithology). On the other hand, it stems from the dialog between a geologist and a geophysicist, which would lead to formalized search criteria based on personal experience. Thus, the most reasonable approach would be to formulate such criteria proceeding from necessary and sufficient conditions in terms of parameters that characterize an object or a process.

Joint inversion itself is neither necessary nor sufficient for obtaining faithful models of reality from geophysical data. The integration approaches may be difficult to apply to data sets, which are acquired at different resolutions and scales or are controlled by different physical processes. In the latter case, it is almost impossible to know *a priori* whether the data represent some correlated structures in the subsurface. Joint inversion is basically simple if all data are sensitive to the same properties, and the resulting model is expected to be at least no worse than those derived from single data sets. However, integration of physically different (e.g., electromagnetic and seismic) data may generally fail, though providing more insights into the subsurface structure, reducing ambiguity, and attenuating noise. Cross-gradient modeling may even "detect" an object that actually does not exist, because the problem formulation originally assumes that all data sets would image some specific structure, even if the parameters correlate poorly. Therefore, evaluation and checking of joint inversion results (against some additional priors) is even more important than in the case of separate inversion.

Posterior joint interpretation of independent inverted data sets appears to be the most reasonable in terms of methodology (at least, free from the above pitfall). It can reveal regions of best correlation between parameters (which may be proxies of different phenomena) or clusters of petrophysical properties related to a certain lithology. Such interpretation has to use the mapped geophysical parameters that are especially sensitive to the target structures or processes, i.e., it has to be preceded by sensitivity analysis within each geophysical method. The cluster models obtained by the posterior joint analysis of level I models can make reference for further more advanced joint inversion of geophysical data.

REFERENCES

Aarst, E., Korst, J., 1989. Simulated Annealing and Boltzman Machines: A Stochastic Approach to Combinatorial Optimization and Neural Computing. Wiley Publ., Chichester.

Abubakar, A., Gao, G., Habashy, T.M., Liu, J., 2012. Joint inversion approaches for geophysical electromagnetic and elastic full-waveform data. Inverse Prob. 28 (5), doi:10.1088/0266-5611/28/5/055016.

Backus, G.E., 1988. Bayesian inference in geomagnetism. Geophys. J. 92, 125–142.

Bauer, K., Pratt, R.G., Haberland, C., Weber, M., 2008. Neural network analysis of crosshole tomographic images: the seismic signature of gas hydrate bearing sediments in the Mackenzie Delta (NM Canada). Geophys. Res. Lett. 35 (19), L19306.

Bauer, K., Muñoz, G., Moeck, I., 2012. Pattern recognition and lithological interpretation of collocated seismic and magnetotelluric models using self-organizing maps. Geophys. J. Int. 189, 984–998.

Bedrosian, P.A., 2007. MT+, integrating magnetotellurics to determine earth structure, physical state and processes. Surv. Geophys. 28, 121–167.

Bedrosian, P.A., Maercklin, N., Weckmann, U., Bartov, Y., Ryberg, T., Ritter, O., 2007. Lithology-derived structure classification from the joint interpretation of magnetotelluric and seismic models. Geophys. J. Int. 170, 737–748.

Bertsimas, D., Tsitsiklis, J., 1993. Simulated Annealing. Statistical Sci. 8 (1), 10–15.

Bosch, M., 1999. Lithologic tomography: from plural geophysical data to lithology estimation. J. Geoph. Res. 104 (B1), 749–766.

Bosch, M., Guillen, A., Ledru, P., 2001. Lithologic tomography: an application to geophysical data from Cadomian belt of northern Brittany, France. Tectonophysics 331, 197–227.

Cerny, V., 1985. Thermodynamical approach to the traveling salesman problem: an efficient simulation algorithm. J. Optim. Theory Appl. 45, 41–51.

Cheremisina, E.N., Galuev, V.I., Kaplan, S.A., Malinina, S.S., 2006. Method for detecting reference interfaces for integration of geological and geophysical data in regional studies. Geoinformatika, No. 1, 50–53.

Dell'Aversana, P., 2001. Integration of seismic, MT and gravity data in a thrust belt interpretation. First Break 6, 335–341.

Dell'Aversana, P., 2006. Joint inversion of seismic, gravity and magnetotelluric data combined with depth seismic imaging. Ext. Abstr. 18th IAGA WG 1.2 Workshop on EM Induction in the Earth, El Vendrell, Spain.

Dell'Aversana, P., 2014. Integrated geophysical models combining rock physics with seismic, electromagnetic and gravity models. EAGE Publ. DB Houten, The Netherlands.

Dell'Aversana, P., Morandi, S., 2002. Depth model building by constrained magnetotelluric inversion. Ann. Geophys. 45 (2), 247–257.

Dell'Aversana, P., Bernasconi, G., Miotti, F., Rovetta, D., 2011. Joint inversion of rock properties from sonic, resistivity and density well-log measurements. Geophys. Prosp. 59 (6), 1144–1154.

Doetsch, J., Linde, N., Coscia, I., Greenhalgh, S.A., Green, A.G., 2010. Zonation for 3D aquifer characterization based on joint inversions of multimethod crosshole geophysical data. Geophysics 75 (6), G53–G64.

Fregoso, E., Gallardo, L.A., 2009. Cross-gradients joint 3D inversion with applications to gravity and magnetic data. Geophysics 74 (4), L31–L42.

Fullea, J., 2017. On joint modelling of electrical conductivity and other geophysical and petrological observables to infer the structure of the lithosphere and underlying upper mantle. Surv. Geophys. 38, 963–1004. doi: 10.1007/s10712-017-9432-4.

Gallardo, L.A., Meju, M.A., 2003. Characterization of heterogeneous near-surface materials by joint 2D inversion of DC resistivity and seismic data. Geophys. Res. Lett. 30 (13), 1658. doi: 10.1029/2003GL017370.

Gallardo, L.A., Meju, M.A., 2007. Joint two-dimensional cross-gradient imaging of magnetotelluric and seismic traveltime data for structural and lithological classification. Geophys. J. Int. 169, 261–1272.

Gallardo, L.A., Meju, M.A., 2011. Structure-coupled multiphysics imaging in geophysical sciences. Rev. Geophys. 49 (1) RG1003. doi: 10.1029/2010RG000330.

Gallardo, L.A., Meju, M.A., Perez-Flores, M.A., 2005. A quadratic programming approach for joint image reconstruction: mathematical and geophysical examples. Inverse Prob. 21, 435–452.

Galuev, V.I., Kaplan, S.A., 2009. Joint interpretation of data within a fragment of the 2-DV transect. Razvedka i Okhrana Nedr 4, 49–56.

Gao, G., Abubakar, A., Habashy, T.M., 2012. Joint petrophysical inversion of electromagnetic and full-waveform seismic data. Geophysics 77 (3), WA3–WA18.

Geman, S., Geman, D., 1984. Stochastic relaxation, Gibbs distribution and the Bayesian restoration of images. IEEE Trans. Pattern Anal. Mach. Intell. 6, 721–741.

Golizdra, G.Ya., 1978. Integration of gravity and seismic data. Izv. AN SSSR, Ser. Fizika Zemli, No. 6, 26–38.

Goltsman, F.M., Kalinina, T.B., 1973. Integration of geophysical data. Izv. AN SSSR. Ser. Fizika Zemli, No. 8, 31–42.

Grandis, H., 1994. Imagerie Électromagnétique Bayesienne par la Simulation d'une Chaine de Markov. Doctoral d'Université, Université Paris VII, Paris.

Habashy, T.M., Abubakar, A., 2004. A general framework for constraint minimization for the inversion of electromagnetic measurements. Progress in Electromagnetic Research Symp. 46, 265–312. doi: 10.2528/PIER03100702.

Haber, E., Oldenburg, D., 1997. Joint inversion: a structural approach. Inverse Prob. 13, 63–77.

Hamdan, H., Economou, N., Kritikakis, G., Andronikidis, N., Manoutsoglou, E., Vafidis, A., Pangratis, P., Apostolidou, G., 2012. 2D and 3D imaging of the metamorphic carbonates at Omalos plateau/polje, Crete, Greece, by employing independent and joint inversion on resistivity and seismic data. Int. J. Speleol. 41 (2), 199–209.

Harris, P., MacGregor, L., 2007. Enhancing the resolution of CSEM inversion using seismic constraints. Expanded Abstr. SEG San Antonio Annual Meeting.

Hartigan, J., 1975. Clustering Algorithms. John Wiley & Sons, New York.

Haupt, R.L., Haupt, S.E., 2004. Practical Genetic Algorithms. Second edition. John Wiley & Sons, Inc., Hoboken, New Jersey.

Hellman, K., Ronczka, M., Gunther, T., Wennermark, M., Rucker, C., Dahlin, T., 2017. Structurally coupled inversion of ERT and refraction seismic data combined with cluster-based model integration. J. Appl. Geophys. 163, 169–181.

Holland, J.H., 1975. Adaptation in Natural and Artificial Systems. University of Michigan Press, Ann Arbor, MI.

Hu, W., Abubakar, A., Habashy, T.M., 2009. Joint electromagnetic and seismic inversion using structural constraints. Geophysics 74 (6), R99–R109.

Huberty, C.J., 1994. Applied Discriminant Analysis. John Wiley & Sons, Inc, New York.

Infante, V., Gallardo, L.A., Montalvo-Arrieta, J.C., de León, I.N., 2010. Lithological classification assisted by the joint inversion of electrical and seismic data at a control site in northeast Mexico. J. Appl. Geophys. 70, 93–102.

JafarGandomi, A., Binley, A., 2013. A Bayesian trans-dimensional approach for the fusion of multiple geophysical datasets. J. Appl. Geophys. 96, 38–54.

Jardani, A., Revil, A., Dupont, J.P., 2013. Stochastic joint inversion of hydrogeophysical data for salt tracer test monitoring and hydraulic conductivity imaging. Adv. Water Resour. 52, 62–77.

Jousset, P., Haberland, C., Bauer, K., Árnason, K., 2011. Hengill geothermal volcanic complex (Iceland) characterized by integrated geophysical observations. Geothermics 40, 1–24.

Kaipio, J.P., Kolehmainen, V., Vauhkonen, M., Somersalo, E., 1999. Inverse problems with structural prior information. Inverse Prob. 15, 713–729.

Kanungo, T., Mount, D.M., Netanyahu, N.S., Piatko, C.D., Silverman, R., Wu, A.Y., 2002. An efficient k-means clustering algorithm: analysis and implementation. IEEE Trans. Pattern Anal. Machine Intelligence 24 (7), 881–892.

Kaplan, S.A., Galuev, V.I., Pimanova, N.N., Malinina, S.S., 2006. Integration of data along transects. Geoinformatika, No. 3, 38–46.

Kaufman, L., Rousseeuw, P.J., 2005. Finding Groups in Data. John Wiley & Sons, London.

Kirkpatrick, S., Gelatt, Jr. C.D., Vecchi, M.P., 1983. Optimization by simulated annealing. Science 220, 671–680.

Kohonen, T., 2001. Self-Organizing Maps. Springer-Verlag, Berlin.

Lelievre, P.G., Farquharson, C.G., Hunch, C.A., 2012. Joint inversion of seismic traveltimes and gravity data on unstructured grids with application to mineral exploration. Geophysics 77 (1), K1–K15.

Lines, L.R., Schultz, A.K., Treitel, S., 1988. Cooperative inversion of geophysical data. Geophysics 53 (1), 8–20.

Lochbuhler, T., Doetsch, J., Brauchler, R., Linde, N., 2013. Structure-coupled joint inversion of geophysical and hydrological data. Geophysics 78 (3), ID1–ID14.

MacCalman, L., O'Callaghan, S.T., Reid, A., Shen, D., Carter, S., Krieger, L., Beardsmore, G., Bonilla, E.V., Ramos, F.T., 2014. Distributed Bayesian geophysical inversions. Expanded Abstr. Thirty-Ninth Workshop on Geothermal Reservoir Engineering, Stanford, California.

Maercklin, N., Bedrosian, P.A., Haberland, C., Ritter, O., Ryberg, T., Weber, M., Weckmann, W., 2005. Characterizing a large shear-zone with seismic and magnetotelluric methods: the case of the Dead Sea Transform. Geoph. Res. Lett. 32 (15), L15303. doi: 10.1029/2005GL022724.

Mellors, R.J., Tompson, A., Dyer, K., Yang, X., Chen, M., Wagoner, J., Trainor-Guiton, W., Ramirez, A., 2014. Stochastic Joint Inversion Modeling Algorithm of Geothermal Prospects. Expanded Abstr. Thirty-Ninth Workshop on Geothermal Reservoir Engineering, Stanford, California.

Moorkamp, M., Jones, A.G., Rao, C.K., 2006. Joint inversion of MT and seismic receiver function data using a genetic algorithm. Ext. Abstr. 18th IAGA WG 1.2 Workshop on EM Induction in the Earth, El Vendrell, Spain.

Moorkamp, M., Jones, A.G., Eaton, D.W., 2007. Joint inversion of teleseismic receiver functions and magnetotelluric data using a genetic algorithm: are seismic velocities and electrical conductivities compatible? Geophys. Res. Lett. 34, L16311. doi:10.1029/2007GL030519.

Moorkamp, M., Jones, A.G., Fishwick, S., 2010. Joint inversion of receiver functions, surface wave dispersion, and magnetotelluric data. J. Geophys. Res. 115, B04318. doi:10.1029/2009JB006369.

Moorkamp, M., Heincke, B., Jegen, M., Roberts, A.W., Hobbs, R.W., 2011. A framework for 3-D joint inversion of MT, gravity and seismic refraction data. Geophys. J. Int. 184, 477–493.

Moorkamp, M., Lelièvre, P.G., Linde, N., Khan, A. (Eds.), 2016. Integrated Imaging of the Earth: Theory and Applications. AGU and John Wiley & Sons, London.

Mosegaard, K., Tarantola, A., 1995. Monte Carlo sampling of solutions to inverse problems. J. Geophys. Res. 100 (B7), 12431–12447.

Mota, R., Monteiro Santos, F.A., 2010. 2D sections of porosity and water saturation from integrated resistivity and seismic surveys. Near Surf. Geophys. 8, 575–584.

Muñoz, G., Bauer, K., Moeck, I., Schulze, A., Ritter, O., 2010. Exploring the Gross Schonebeck (Germany) geothermal site using a statistical joint interpretation of magnetotelluric and seismic tomography models. Geothermics 39, 35–45.

Nikitin, A.A., Kaplan, S.A., Galuev, V.I., Malinina, S.S., 2003. Physico-geometrical properties of the crust inferred from integrated geophysical data. Geoinformatika 2, 29–38.

Paasche, H., Tronicke, J., Dietrich, P., 2012. Zonal cooperative inversion of partially co-located data sets constrained by structural *a priori* information. Near Surface Geophysics 10, 103–116.

Pinheiro, P.A.T., Loh, W.W., Dickin, F.J., 1997. Smoothness-constrained inversion for two-dimensional electrical resistance tomography. Meas., Sci. Technol., 8, 293–302.

Press, S.J., 2002. Subjective and Objective Bayesian Statistics: Principle, Models, and Applications. John Wiley & Sons, London.

Rasmussen, C.E., Williams, C.K.I., 2006. Gaussian Processes for Machine Learning. The MIT Press, Cambridge, London.

Reimann, C., Filzmoser, P., Garrett, R., Dutter, R., 2008. Statistical Data Analysis Explained. John Wiley & Sons, London.

Ren, H., Ray, J., Hou, Z., Huang, M., Bao, J., Swiler, L., 2017. Bayesian inversion of seismic and electromagnetic data for marine gas reservoir characterization using multi-chain Markov chain Monte Carlo sampling. J. Appl. Geophys., 147, 68–80. doi: 10.1016/j.jappgeo.2017.10.004.

Roussignol, M., Jouanne, V., Menvielle, M., Tarits, P., 1993. Bayesian electromagnetic imaging, in: Hardle, W., Siman, L. (Eds.), Computer Intensive Methods. Physical Verlag, pp. 85–97.

Sambridge, M., Mosegaard, K., 2002. Monte Carlo methods in geophysical inverse problems. Rev. Geophys. 40 (3), 1009. doi:10.1029/2000RG000089.

Saunders, J.H., Herwanger, J.V., Pain, C.C., Worthington, M.N., de Oliveira, C.R.E., 2005. Constrained resistivity inversion using seismic data. Geoph. J. Int. 160, 785–796.

Spichak, V.V., 2005. 3D Bayesian inversion, in: Electromagnetic Surveys [in Russian], Nauchnyi Mir, Moscow, p. 91–109.

Spichak, V.V., 2009. Modern approaches to joint inversion of geophysical data. Geofizika 5, 10–19.

Spichak, V.V., 2010. Methods for integration of electromagnetic and other geophysical data, in: Integrated Analysis of Electromagnetic and Other Geophysical Data [in Russian], LIBROKOM, Moscow, pp. 6–28.

Spichak, V.V., Menvielle, M., Roussignol, M., 1999. Three-dimensional inversion of EM data using Bayesian statistics, in: Spies, B., Oristaglio, M. (Eds.), 3D Electromagnetics, SEG Publ. GD7. Tulsa. USA, pp. 406–417.

Spichak, V., Rybin, A., Batalev, V., Sizov, Y., Zakharova, O., Goidina, A., 2006. Application of ANN techniques to combined analysis of magnetotelluric and other geophysical data in the northern Tien Shan crustal area. Ext. Abstr. 18th IAGA WG 1.2 Workshop on EM Induction in the Earth, El Vendrell, Spain.

Spichak, V.V., Borisova, V.P., Fainberg, E.B., Khalezov, A.A., Goidina, A.G., 2007. 3D electromagnetic tomography of the Elbrus volcanic center with reference to magnetotelluric and satellite data. J. Volcan. Seismol. 1, 58–73.

Spichak, B.B., Bezruk, I.A., Popova, I.V., 2008. Petrophysical interpretation of geophysical data and prediction of basin potential. Geofizika 5, 43–45.

Spichak, V.V., Bezruk, I.A., Goidina, A.G., 2015. 3D cluster petrophysical modeling using integrated geophysical data along transects. Razvedka i Okhrana Nedr 4, 41–45.

Tarantola, A., 1987. Inverse Problem Theory: Method for Data Fitting and Model Parameter Estimation. Elsevier, New York, 613 pp.

Tondi, R., Cavazzoni, C., Danecek, P., Morelli, A., 2012. Parallel, 'large', dense matrix problems: Application to 3D sequential integrated inversion of seismological and gravity data. Comput. Geosci. 48, 143–156.

Zhu, T., Harris, J.M., 2011. Iterative joint inversion of *P*-wave and *S*-wave crosswell traveltime data. Expanded Abstr. SEG San Antonio Annual Meeting, pp. 479–483.

Editorial responsibility: A.D. Duchkov